sciendo

Green Sciences, 27, 4, 34—45, 10.2478/pjct-2025-0019

Effect of Poly (2-hydroxyethyl methacrylate) on the Release of Phenylacetaldehyde from Chitosan Matrix

Fethia Benmerad[1], Hassiba Benguergoura[2], Soufiane Rahal[3], Taieb Aouak[4]

[1]Chimie Physique des Interfaces des Matériaux Appliqués à l'Environnement CPIMAE, Université Blida 1, B.P.520 route de Soumaa, Blida, Algeria
[2]Laboratoire eau, environnement et développement durable (EEDD), Université Blida 1, B.P.520 route de Soumaa, Blida, Algeria
[3]Biomaterials and Transport Phenomena Laboratory (LBMPT), Université Yahia Fares Medea, street Aïnd'Heb, 526000, Algeria
[4]Chemistry Department, College of Science, King Saud University, P.O. Box 2455, Riyadh 11451, Saudi Arabia.
[*]*Corresponding author:* e-mail: benmerad_fethia@univ-blida.dz

To investigate the effect of Poly (2-hydroxyethyl methacrylate) on the extended release of Phenylacetaldehyde, considered as a prototype of drug with aldehyde function, tow series of chitosan (CS) based systems were prepared; graft compolymers Chitosan-Phenylacetaldehyde–*graft*-poly(2-hydroxyethylmethacrylate) [CSPhAcAl-*graft*-PHEMA] with various PhAcAL ratios, and blends consisting of Chitosan-phenylacetaldehyde/ Poly(2-hydroxyethylmethacrylate) [CSPhAcAl/PHEMA] with different PHEMA. PhAcAl was covalently attached to chitosan CS via Schiff base reaction assisted by pervaporation. FTIR and 1HNMR analyses confirmed chitosan Schiff base formation and its graft copolymerization with PHEMA, while distribution of PhAcAl within the copolymer matrix was examined using XRD and DSC analysis. Both systems exhibited pH-responsive swelling, however, significant differences were observed in their release behavior. CSPhAcAl/ PHEMA systems with 3.74 and 8.98 wt% of PhAcAl content demonstrated the highest performance at pH 7. The release kinetics of the grafted systems followed the Korsmeyer-Peppas and Higuchi models, suggesting a Fickian diffusion-controlled mechanism. In contrast, blended systems demonstrated mixed behavior.

Keywords: chitosan, Poly (2-hydroxyethyl methacrylate), functional polymers, Schiff base based materials, extended delivery.

Received: 29 July 2025; Accepted: 14 November 2025; Available online: 14.01.2026.

INTRODUCTION

To address the challenges posed by conventional drug delivery systems, such as low bioavailability, short biological half-life, and drug resistance requiring frequent or high doses that often lead to significant side effects, scientists have turned their attention to synthetic polymers, which are developed as polymeric drugs or advanced drug delivery systems to enhance therapeutic outcomes[1, 2].

Polymeric drug carriers are specific polymers that incorporate active substances either as pendant or terminal groups, allowing therapeutic agents attached to a polymeric backbone to achieve prolonged blood circulation, controlled release, enhanced pharmacokinetics, improved solubility, reduced toxicity, and targeted delivery to specific tissues[3]. To ensure such controlled and site-specific release, the choice of an appropriate linker becomes crucial; it must be strong enough to prevent premature drug release while being sensitive to enzymatic activity or pH changes to ensure release at the desired site. Among the different linker reactions used in chemical research, the Schiff-base (SB) reaction, a type of dynamic covalent reaction, stands out for its simplicity, reversibility, and ease of preparation. The imine bond, in the Schiff base structure, can undergo hydrolytic cleavage under acidic conditions, enabling controlled drug release, which makes SB linkages particularly attractive for various biomedical and pharmaceutical applications[4–8].

Schiff base systems that are based on chitosan (CSB) are being increasingly valued for drug delivery systems because they are biocompatible, biodegradable, and pH--responsive. Several CSB hydrogels have been reported to provide sustained delivery of antibiotics and anticancer drugs, such as chitosan- cuminaldehyde hydrogels, which prolonged levofloxacin delivery, or gather CS-dihydrocaffeic acid systems that delivered doxorubicin and amoxicillin in a therapeutic time frame with antibacterial and antitumor efficacy[7–10]. In some cases, prototypical model drugs such as vanillin are used instead of actual drugs[11].

In this study, two phenylacetaldehyde (PhAcAl) containing carrier systems were prepared by grafting PhAcAl onto chitosan (CS) with a Schiff base reaction, using the pervaporation technique, a versatile method that can promote equilibrium-driven reactions, to eliminate water byproduct[12]. In the first system, CSPhAcAl was graft-copolymerized with 2-hydroxyethyl methacrylate (HEMA), whereas in the second, it was physically blended with poly(2-hydroxyethyl methacrylate) (PHEMA), a hydrophilic, biocompatible, and FDA-approved polymer widely applied in various biomedical fields, and drug delivery[13–15]. Its incorporation in chitosan Schiff base systems improves mechanical strength, elasticity, and film-forming ability while controlling swelling to achieve steady drug release and reduce burst release[16].

Phenylacetaldehyde (PhAcAl) was chosen as a model aldehydic drug due to its reactive carbonyl functionality, low molecular weight, and medium aqueous solubility, which allow for homogeneous dispersion in the chitosan matrix. The presence of an aromatic ring gives rise medium hydrophobicity and electron delocalization.

A comparison of these two approaches demonstrates the strong influence of PHEMA inclusion, either chemically or physically, on the release behavior of aldehyde-containing molecules. This two-part approach is a promising platform for the manufacture of chito-

san-drug carriers for drugs that contain aldehydes such as vitamin A, vitamin B6, certain antibiotics such as spiramycin and streptomycin, and paraldehyde, which has been used in the management of insomnia[3].

MATERIALS AND METHODS

Chemicals

Phenylacetaldehyde (PhAcAl) (purity ≥ 90%), 2-hydroxyethylmethacrylate (HEMA) (purity 99%), ammonium persulfate (APS) (purity, 98%) was supplied by Sigma Aldrich (Germany). Chitosan (CS) with an average molecular weight of 200,000 g/mol and a deacetylation degree of about 90% was obtained from Jakwang Co., Korea. All chemicals were used as received without any prior purification.

Synthesis of CSPhAcAl

Phenylacetaldehyde was grafted onto chitosan through a Schiff base reaction between the amine group of CS and the aldehyde function of PhAcAl, as shown in Scheme 1.

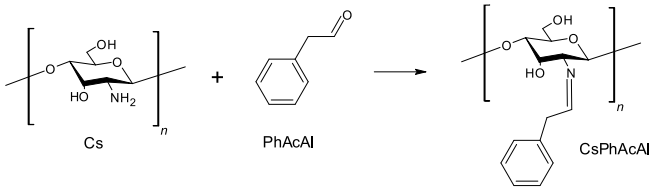

Scheme 1. Grafting reaction of Phenylacetaldehyde (PhAcAl) onto Chitosan (Cs)

A known amount of chitosan dissolved in 50 mL of a 2-volume acetic acid/methanol solution was placed in the upstream section of a pervaporation cell[12], equipped with a hydrophilic poly (vinyl alcohol) membrane. Phenylacetaldehyde was then added dropwise to the chitosan solution under stirring at 70 °C using a separating funnel. Samples of 2 mL were taken every 2 h using a glass hypodermic syringe. The grafted chitosan obtained at the end of the reaction was purified by washing three times with water, then re-dissolved again in chloroform, precipitated in heptane, and dried under vacuum at 40 °C until a constant weight was achieved.

To create films of the resulting material, a known amount of CSPhAcAl varying from 5 to 20% (wt%), was dissolved in a solvent mixture of acetic acid and methanol, then poured into a horizontally maintained Teflon mold and allowed to dry at ambient temperature for 24 h, followed by vacuum drying at 40 °C until a constant weight was reached. A series of four CSPhAcAl films CSPhAcAl 3, CSPhAcAl 6, CSPhAcAl 10, CSPhAcAl 15, containing 3.75, 8.98, 9.52, and 15.40 mol% of PhAcAl, respectively, were prepared (percentages determined by ^{1}HNMR method described in Section 3.1.2). Film thickness was determined using a micrometer and found to range between 233 and 247 μm.

Synthesis of CSPhAcAl-*graft*-PHEMA

Grafting copolymerisation of CSPhAcAl and HEMA (Scheme 2) was performed as follows, in a three-necked flask, a known amount of dry CSPhAcAl was dissolved in distilled water. HEMA and APS were then added subsequently to the solution while stirring moderately at 25 °C until complete dissolution. A condenser was connected to the central neck of the flask, and the other two necks were fitted with a thermometer and a nitrogen gas inlet (with a flow rate of 3 ml/min). Once the copolymerization reaction is complete, indicated by the formation of a highly viscous solution, the reaction mixture is then precipitated by pouring it into an excess of acetone, filtered through a Buchner funnel, and subsequently rinsed multiple times with acetone to remove any unreacted HEMA. The resulting powder was air-dried for 24 h and then further dried under vacuum until a constant weight was achieved. The ratio [CSPhAcAl: HEMA] for each copolymer is equal to [1:1].

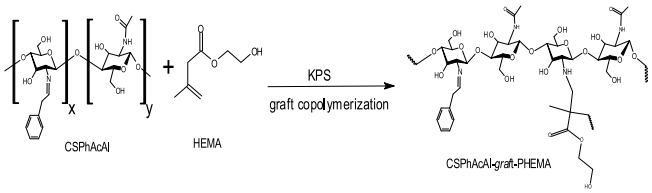

Scheme 2. Grafting copolymerization of HEMA on CSPhAcAl

Synthesis of the CSPhAcAl/PHEMA blend

CSPhAcAl was dissolved in 20 mL of a 2-volume acetic acid/ methanol solvent mixture. In a separate preparation, a known amount of PHEMA was dissolved in an equivalent volume of pure methanol. The two solutions were then mixed together under stirring, and the resulting mixture was poured into a Teflon mold and allowed to dry at ambient temperature for 24 h, followed by vacuum drying at 40 °C until a constant weight was reached. Different blends containing various PHEMA and CSPhAcAl ratios were synthesized as shown in Table 1.

Table 1. Compositions of CSPhAcAl/PHEMA blends with different PHEMA content

Blends	CSPhAcAl (wt %)	PHEMA (wt %)
CSPhAcAl /PHEMA3.74	12	88
CSPhAcAl /PHEMA8.98	26	74
CSPhAcAl /PHEMA9.52	27	73
CSPhAcAl /PHEMA15.40	39	61

Characterization

The structures of PhAcAl, CSPhAcAl, CSPhAcAl-*graft*--PHEMA, and CSPhAcAl/PHEMA were characterized using Fourier-transform infrared spectroscopy (FTIR) and nuclear magnetic resonance (NMR) spectroscopy. The thermal properties of the copolymers and composites were investigated using differential scanning calorimetry (DSC).

FTIR Analysis

FTIR spectra of the different prepared materials were recorded using a Perkin Elmer Spectrum GX FTIR spectrometer (USA) operating in attenuated total reflectance mode, within a wavenumber range of 4000 to 650 cm^{-1}, with a resolution of 2 cm^{-1}. The samples were analysed as thin films deposited on dehydrated NaCl plates.

XRD Analysis

XRD patterns of the synthesized materials with different compositions were collected using a BRUKER D8 Advanced diffractometer (Germany). The measurements

were performed with Cu Kα radiation at 40 mA and 40 kV, with a scanning rate of 2°/min in 2θ.

DSC Analysis

DSC thermograms of the prepared products were recorded using a DSC apparatus (Shimadzu DSC 60, Japan), previously calibrated with indium. Samples weighed between 10 and 12 mg were packed in DSC aluminium capsules then heated between –100 °C and 350 °C. The glass transition temperature (Tg) was determined from the inflection point of the polymer's glass transition, and the melting temperature was obtained from the top of the endothermic peak corresponding to the fusion enthalpy of the sample.

Swelling studies

Swellable matrices are activated by water, and drug release control depends on the interactions between water, polymer, and drug. Water penetration into the matrix is the first step leading to swelling and polymer and drug dissolution[17].

The swelling behavior of a polymer is then a key factor in understanding how a drug is released from its delivery system. This property is influenced by several factors, including the degree of crosslinking within the polymer matrix, the temperature and the pH of the release medium, and the types of chemical bonds that may form during polymer grafting or blending[18–22].

To explore how polymeric drug carriers behave when exposed to biological fluids, we conducted a swelling study on the prepared materials CSPhAcAl-*graft*-PHEMA, and CSPhAcAl/PHEMA as well as pure Cs and pure PHEMA. Pieces of dry films were immersed in acidic solutions for pH 1 and 3, and in phosphate-buffered saline (PBS) solutions for pH 5 and 7, at 37 °C. Then, at certain time intervals, the swollen samples were withdrawn, and the excess of water was quickly wiped with tissue paper. Swelling was considered complete (equilibrium) when the sample's weight no longer changed over time. Swelling percentage (%) is then calculated using Equation (1):

$$S(\%) = \frac{w_t - w_0}{w_0} \times 100 \quad (1)$$

where w_0 and w_t are the weights of the swollen and dry films, respectively.

In Vitro Drug Release

CSPhAcAl-*graft*-PHEMA copolymers and CSPhAcAl/PHEMA blends in film forms were placed in a beaker containing an acetic acid aqueous solution maintained at a constant pH and stirred at 130 rpm in a thermostatic bath at 37 °C. This experiment was conducted at pH levels of 1, 3, 5, and 7. Aliquots of 0.5 mL were taken at specified time intervals; each aliquot removed was immediately replaced with an equivalent volume of the acetic acid aqueous solution of the same concentration. The amounts of PhAcAl released from the synthesized materials were determined using an Aultropec 2100 pro UV-visible spectrophotometer from Amersham Biosciences at 281 nm, employing a PhAcAl calibration curve in a methanol-water solvent mixture. The release experiments were conducted at 37 °C with medium pH values of 1, 3, 5, and 7. The cumulative release of PhAcAl was determined using the standard absorbance curve obtained from UV analysis, in accordance with Equation (2).

$$R(wt\%) = \frac{m_t}{m_0} \times 100 \quad (2)$$

where m_t and m_0 represent the mass of PhAcAl released into the medium at time t and at t_0, respectively.

Drug release kinetics

To better understand the release behavior of the synthesized materials, four kinetic models, zero-order (Equation (3)), first-order (Equation (4)), Higuchi (Equation (5)), and Korsmeyer-Peppas (Equation (6)), were applied to analyze the phenylacetaldehyde release data using DD Solver, a Microsoft Excel-based add-in program. The coefficient of determination (R^2) was calculated for each model, and the model showing the highest R^2 value (close to 1) was considered the most appropriate and best-fitting model to describe the release kinetics and mechanism.

$$Q_t = K_0\, t \quad (3)$$

Where K_0 is the zero order rate and Q_t is the amount of drug released at time t[23].

$$log\ Q = log\ Q_0 - K_t t\ 2.303 \quad (4)$$

Where Q is the remaining drug in the formulation after time t, Q_0 is the concentration of drug at time t = 0, and K_t is the first-order rate constant[24].

$$Q_t = K_H (t)^{1/2} \quad (5)$$

where, K_H is Higuchi rate constant and Qt is the amount of drug released at time t[25]

$$F = M_t/M = K_m t^n \quad (6)$$

F = fraction of drug released at time't', Mt = amount of drug released at time 't' , M = total amount of drug in dosage form, Km= kinetic constant, n = diffusion or release exponent, t = time in hrs, 'n' = Linear regression of log (Mt / M) versus log t

An *n* value ≤ 0.5 indicates a purely Fickian diffusion mechanism, whereas *n* values between 0.5 and 1 suggest a non-Fickian (anomalous) transport mechanism[24, 25].

RESULTS AND DISCUSSION

Characterization

FTIR

The structures of the different prepared materials, PhAcAl, CSPhAcAl, CSPhAcAl–*graft*-PHEMA, and CSPhAcAl/PHEMA were confirmed through FTIR analysis in the following sequences:

CSPhAcAl

The CSPhAcAl structure was confirmed through comparison of its spectrum with those of its two starting components, chitosan and phenylacetaldehyde, as shown in Figure 1.

The spectrum confirms the chemical structure of the copolymer through the appearance of an absorption band corresponding to the imine group (-C=N-) at 1632.18 cm^{-1}, resulting from the Schiff base reaction

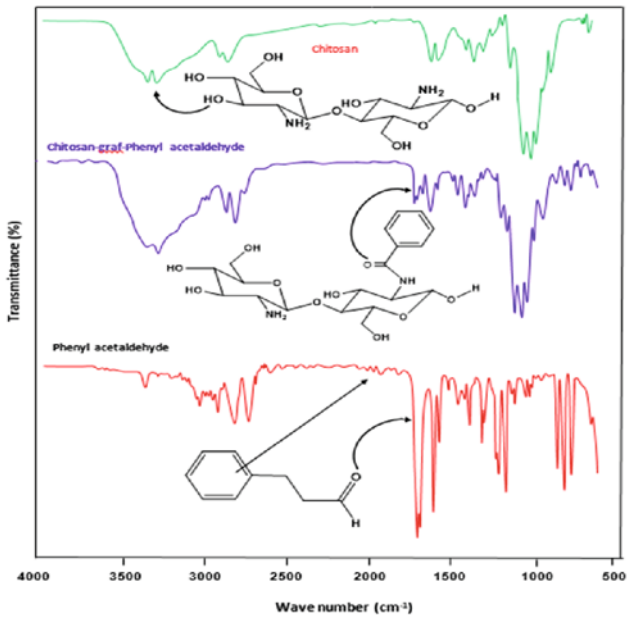

Figure 1. Comparative FTIR spectra of CSPhAcAl and its individual components: chitosan and phenylacetaldehyde

between one or two amino groups of chitosan and the carbonyl group of phenylacetaldehyde. Similar findings have also been reported, confirming the formation of the –C=N– function following the grafting of sulfamethoxazole onto a poly(acrylic acid-co-methyl vinyl ketone)[4].

The CSPhAcAl spectrum displays absorption peaks in the ranges of 1150–1115 cm^{-1}, 1063–1022 cm^{-1}, and 954–895 cm^{-1}, attributed to the saccharide moiety. Additional bands in the regions 1491–1449 cm^{-1}, 750.06 cm^{-1}, and 690.08 cm^{-1} are characteristic of phenyl group absorbance. Finally, the peak at 1733.37 cm^{-1} corresponds to the carbonyl (C=O) function. These absorption bands strongly support the formation of the Schiff base and are in good agreement with the literature[10].

CSPhAcAl-*graft*-PHEMA

Figure 2 shows the FTIR spectrum of CSPhAcAl-*graft*--PHEMA along with PHEMA and CSPhAcAl. The spectrum of PHEMA reveals characteristic peaks at 1745.12 cm^{-1} and those between 1321.0 and 1023.0 cm^{-1}, attributed to the carbonyl stretching vibration of the ester group (-CO-O-) and the ether group (-O-CH_2-), respectively. The broad band appearing at 3542 cm^{-1} is assigned to the hydroxyl group of the substituent (-CH_2-OH), while the peaks between 2930 and 3010 cm^{-1} are attributed to the C-H stretching vibrations of the methyl (-CH_3) and ethyl groups (-CH_2-) in the main chain. The comparison of the FTIR spectrum of CSPhAcAl-*graft*-PHEMA with those of its components confirms the structure of the copolymer. A decrease in the intensity of the absorption band at 1589 cm^{-1}, which is associated with the reaction of NH_2 groups with the carbonyl groups of PhAcAl, leading to the Schiff base formation. Notable changes include the reduction and shift of the absorption band at 1589 cm^{-1} to higher wavenumbers, as well as the broadening and shift of the carbonyl absorption band of PhAcAl and HEMA units, initially localized at 1735.06 cm^{-1}, to lower wavenumbers. This shift has also been observed in the characterization of poly(2-hydroxyethylmethacrylate-co-methylmethacrylate)/lignocaine[26], and poly(2-hydroxyethylmethacrylate–co-cellulose)[27].

Additionally, in the hydroxyl/amine absorption region (2000–4000 cm^{-1}), the peak attributed to chitosan shifted toward the higher wavenumbers following its grafting copolymerization with PHEMA. This shift is attributed to hydrogen bonding interactions between the hydroxyl groups of CS and HEMA units. These observations confirm the chemical structure of the prepared CSPhAcAl-*graft*-PHEMA copolymer. The differences between the spectra of CSPhAcAl and CSPhAcAl-*graft*-PHEMA indicate that PhAcAl is uniformly dispersed at the molecular level within the carrier matrix.

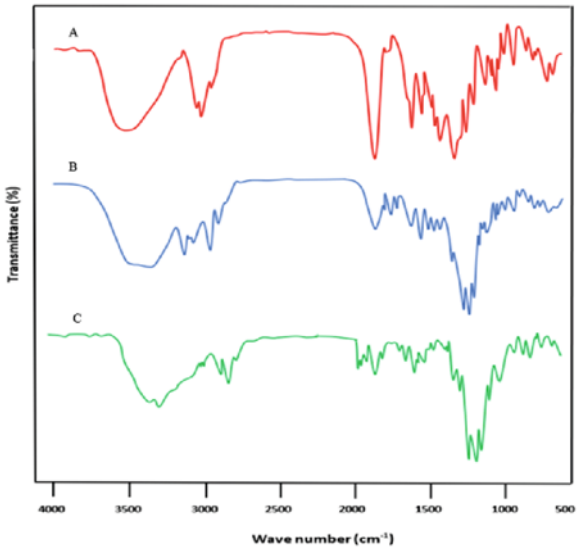

Figure 2. FTIR spectra of PHEMA(A), CSPhAcAl-graft-PHEMA (B) and CSPhAcAl (C)

CS-graft-PhAcAl/PHEMA

The FTIR analysis of the CSPhAcAl/PHEMA blends is showed in Figure 3 and reveals hydrogen bond interactions between CSPhAcAl and PHEMA. These spectra show a shift in the hydroxyl group absorption bands of the HEMA units from 3565.12 cm^{-1} to 3492.21 cm^{-1}, and in the CS units within the CSPhAcAl from 3400.43 cm^{-1} to 3465.02 cm^{-1}. Additionally, the carbonyl band of the HEMA units in pure PHEMA, which appears at 1735.55 cm^{-1}, also shows a shift toward lower wavenumbers. These changes confirm the miscibility of the CSPhAcAl/PHEMA blend system within the investigated compositions.

^{1}HNMR Analysis

CSPhAcAl

The chemical structure of CSPhAcAl was confirmed by ^{1}H NMR as shown in Figure 4. It combines the signals of both components, chitosan and phenylacetaldehyde, such as the benzene ring signals of PhAcAl around 7.32 ppm and the (CH_3-O-) signals of CS between 2.09 and 2.11 ppm. However, new signals appear between 6.4 and 6.6 ppm, corresponding to the protons of the imine group (CH_2-N=CH-), resulting from the Schiff base reaction. Further evidence for the chemical structure of CS-*graft*--PhAcAl is provided by the disappearance of the signal at 9.7 ppm, which is attributed to the aldehyde proton (1) of the PhAcAl[28].

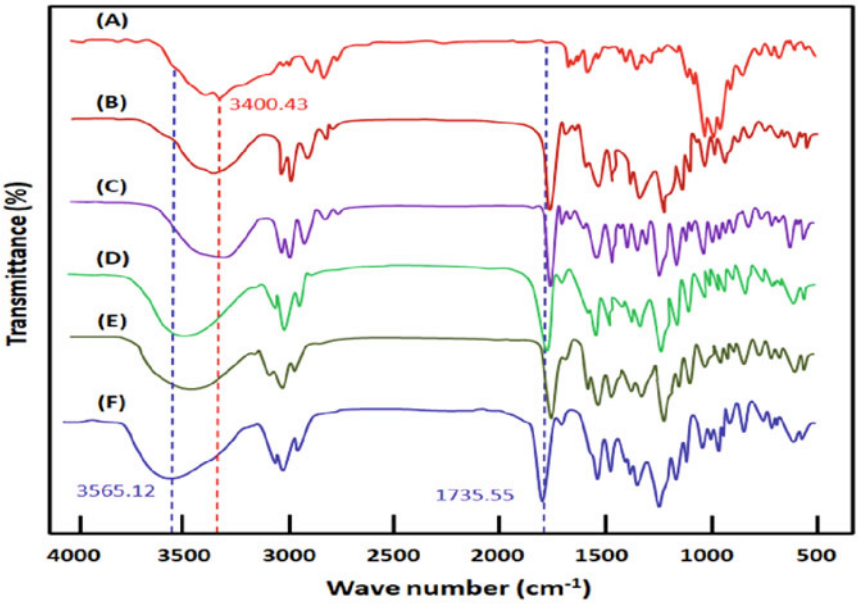

Figure 3. FTIR spectra of: CSPhAcAL (A), and their blends CSPhAcAl/PHEMA containing: (B) 15.40%; (C) 9.52%; (D) 8.98%; (E) 3.75 mol% of CSPhAcAl, and PHEMA (F)

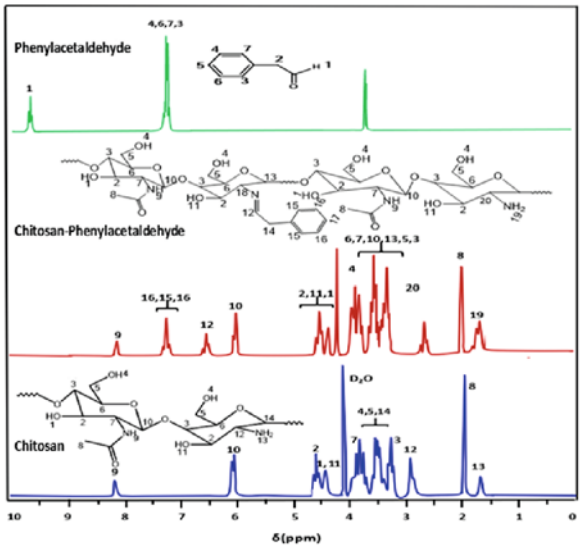

Figure 4. [1]H NMR Spectra of chitosan (CS), phenylacetaldehyde (PhAcAl) and chitosan-phenylacetaldehyde (CSPhAcAl)

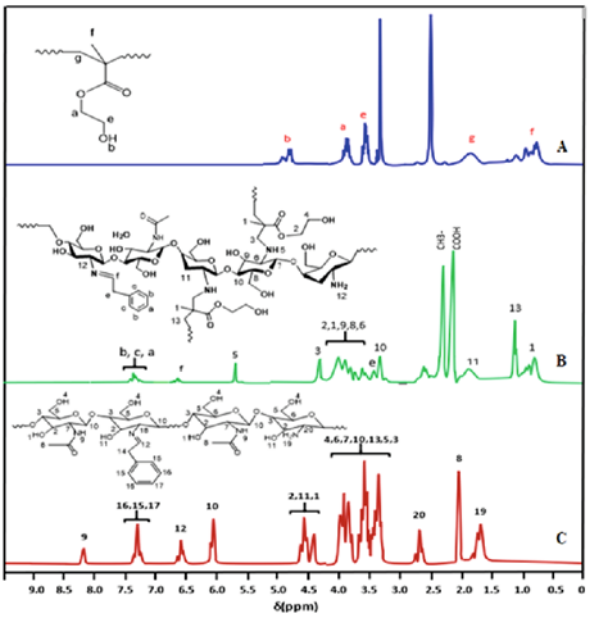

Figure 5. Comparative [1]H NMR Spectra of CSPhAcAl-*graft*--PHEMA (B) with its components CSPhAcAl (C) and PHEMA (A)

CSPhAcAl-*graft*-PHEMA

The spectrum of PHEMA in Figure 5, reveals four characteristic signals. The signal at 3.95 ppm corresponds to the two protons of the ethylene group (-CH_2-) (a), while the second signal at 3.68 ppm is attributed to the two protons of ethylene group (-CH_2-) (e). The signal corresponding to the two ethylene protons (g) on the main chain appears at 1.82 ppm, and the signal for the methyl group (f) is observed between 0.3 and 0.75 ppm. In contrast, the spectrum of PhAcAlCS-*graft*-PHEMA shows, in addition to the signals of both PHEMA and CSPhAcAl, a new signal (3) which appears at 4.25 ppm corresponds to the ethylene group (-CH_2-) adjacent to the NH group, and a signal (5) at 5.65 ppm attributed to NH between CS and PHEMA, thus confirming the structure of PhAcAlCS-*graft*-PHEMA molecule.

The compositions of CSPhAcAl-*graft*-PHEMA in terms of CS, PhAcAl, and PHEMA units were determined through [1]H NMR analysis by integrating the areas of specific signals in the CSPhAcAl-*graft*-PHEMA spectrum. The calculation of these compositions involved determining the areas corresponding to the two ethylene protons (11) in CS and the three protons of the methyl group (-CH_3) (1) in the HEMA monomer using Equation (7). The results obtained are summarized in Table 2.

$$HEMA\ (\%) = \frac{2area_{CH3}(1)}{2\text{area}_{CH3}(1)+3\text{area}_{CH2}(11)} \times 100 \qquad (7)$$

where δarea$_{CH3}$(1), et δarea$_{CH2}$(11) represent the areas of the signals assigned to the –CH_3 groups of HEMA and the –CH_2 groups of CS, respectively.

DSC Analysis

CSPhAcAl

Figure 6 shows the DSC thermograms of CSPhAcAl, CS and PhAcAl.

Table 2. Composition of CSPhAcAl-*graf*-PHEMA obtained by ^{1}HNMR

Systems	PhAcAl (mole%)	CS (mole%)	PHEMA (mole%)
CSPhAcAl 3-*graft*-PHEMA	3.74	45.89	50.37
CSPhAcAl 6-*graft*-PHEMA	8.98	37.02	54.00
CSPhAcAl 10-*graft*-PHEMA	9.52	40.37	50.11
CSPhAcAl 15-*graft*-PHEMA	15.40	48.84	35.76

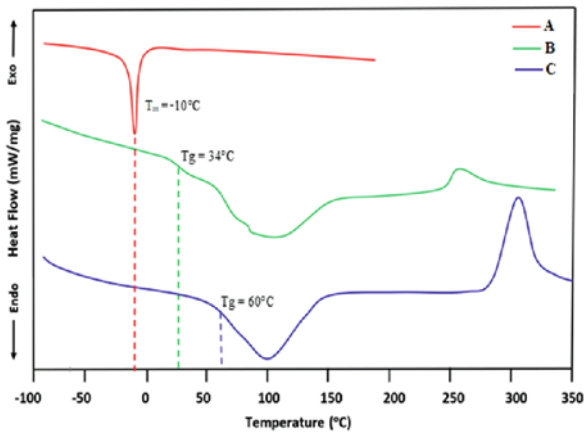

Figure 6. DSC thermograms of PhAcAl (A), CSPhAcAl (B), and CS (C)

The endothermic peak of PhAcAl, which corresponds to the melting temperature of this compound, is observed at –10 °C. As can be seen from the DSC thermogram of pure CS, the Tg value is localized at about 60 °C. According to the literature, Tg value of this biopolymer is controversial; indeed, various Tg values have been reported. According to Mucha and Pawlak, the Tg of CS ranges between 156 and 170 °C, depending on the degree of deacetylation (DDA)[29]. Sakurai estimated it to be 203 °C[30]. Quijada-Garrido observed it at 85 °C[31], while Dong evaluated it to be between 140 and 150 °C[32]. The Tg value of CSPhAcAl is around 34 °C, and the intensity of the melting temperature of CS, which is observed at 302 °C, significantly decreased after the incorporation of PhAcAl into the CS molecule. This results in a marked reduction in the crystallinity of the CS.

CSPhAcAL-graft-HEMA

Figure 7 shows the DSC thermograms of the CSPhAcAl-*graft*-PHEMA with different PhAcAl contents. As can be seen on these thermal curves, only a single Tg for all compositions is observed, the complete disappearance of the melting temperature of the pure PhAcAl at –10 °C, and a shift of Tg value to higher temperatures due to the incorporation of HEMA units into CSPhAcAl. This significantly reduces the chain sliding, leading to an increase in the Tg value of the CSPhAcAl as observed by Alghamdi et al.[4]. These observations suggest that PhAcAl has completely reacted with the CS. The Tg values of the CSPhAcAl-*graft*-HEMA systems with different PhAcAl contents are summarized in Table 3.

CSPhAcAl/PHEMA

The presence of a single Tg, that is intermediate or higher than that of the pure constituents in a binary polymer blend, indicates its miscibility[33, 34]. In this work, miscibility of the CSPhAcAl/PHEMA blend was assessed using DSC method by identifying a single Tg on its thermogram, as shown in Figure 8, which falls between those of the two pure components.

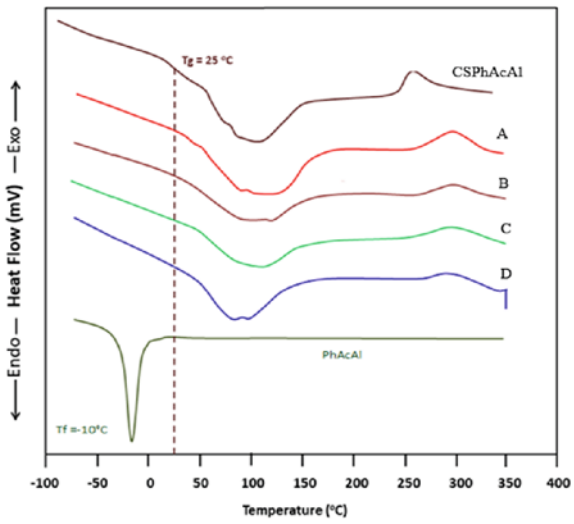

Figure 7. DSC thermograms of CSPhAcAl-*graft*-PHEMA with different PhAcAl contents: CSPhAcAl-*graft*--PHEMA3.74 (A), CSPhAcAl-*graft*-PHEMA8.98 (B), CSPhAcAl-*graft*-PHEMA9.52(C), CSPhAcAl-*graft*--PHEMA15.40 (D)

Table 3. Tg values of the CSPhAcAl-*graft*-PHEMA with different PhAcAl contents

Systems	Tg °C
CSPhAcAl-*graft*-PHEMA3.74	44
CSPhAcAl-*graft*-PHEMA8.98	46
CSPhAcAl-*graft*-PHEMA9.52	50
CSPhAcAl-*graft*-PHEMA15.40	51

X-ray Diffraction Analysis

The X-ray diffractogram of CS in Figure 9 displays three principal reflection signals centred at 10.00°, 19.86°, and 30.00°, confirming the crystalline structure of the polymer, in agreement with previous studies[35]. In contrast, PHEMA exhibits an amorphous nature characterized with two broad signals centred at 13.7° and 30°, consistent with literature findings[13, 36, 37].

For CSPhAcAl, a comparison of the spectra of the pure components with that of the copolymer reveals the

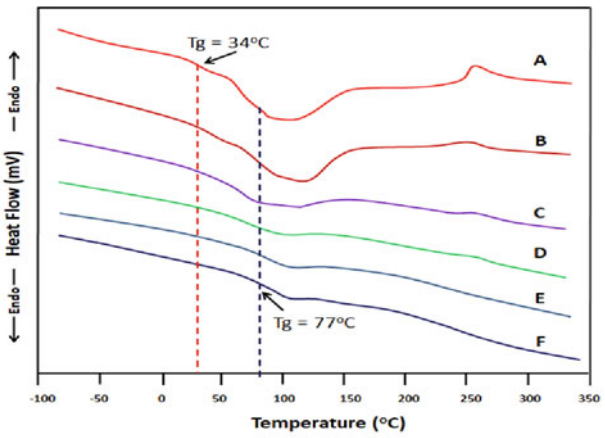

Figure 8. DSC thermogrammes of CSPhAcAl (A), PHEMA(F) and the blend CSPhAcAl /PHEMA containing: (B) 15.40 mol%; (C) 9.52 mol%; (D) 8.98 mol%; (E) 3.74 mol% of CSPhAcAl

complete disappearance of the characteristic crystalline signals of chitosan. This is attributed to the reduction in amine groups and the disruption of hydrogen bonds, corroborating the DSC analysis results, which indicate the absence of the endothermic peak associated with the melting of chitosan.

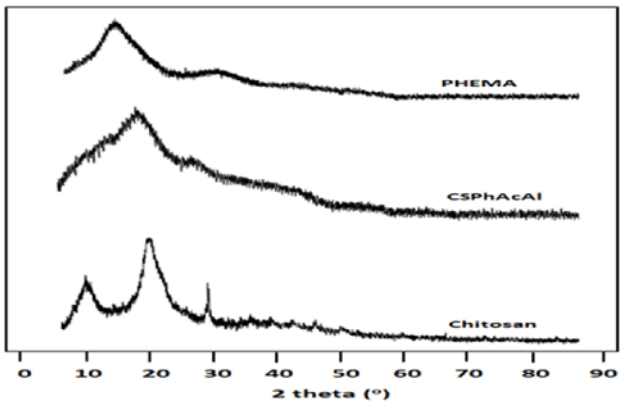

Figure 9. X-ray diffraction spectra of CSPhAcAl, PHEMA and CS homopolymers

The X-ray pattern of the CS/PHEMA blend in Figure 10, demonstrates that after the addition of PHEMA to CS, the crystallographic properties of CS are preserved, as indicated by the unchanged positions of the signals associated with the crystalline structure of CS. This suggests that CS did not react with PHEMA.

Swelling studies

The drug release duration in delivery systems is fundamentally governed by the swelling capacity of the carrier

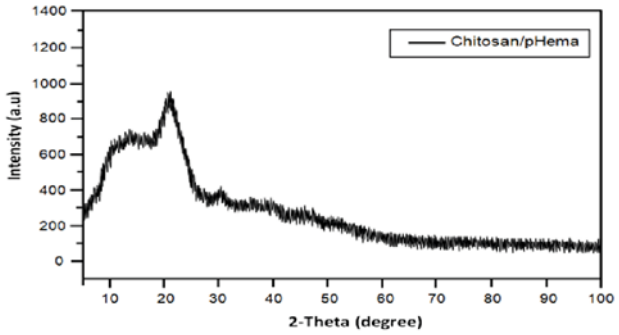

Figure 10. X-ray diffraction spectra of CS/PHEMA blend

matrix. A lower swelling capacity restricts water uptake, subsequently limiting drug dissolution and extending the release profile. The swelling behavior of the CS-*graft*--PHEMA copolymer, CS/PEHMA blend, along with PHEMA and CS, was investigated over time at 37 °C. Analysis of the swelling curves in Figure 11 shows that they exhibit an exponential kinetic profile for all the studied systems, with a rapid initial increase of the swelling degree within the first 30 minutes, followed by stabilization at approximately 2 hours. Additionally, the swelling capacity of all systems was found to increase with decreasing pH, indicating a pronounced pH sensitivity.

It can also be seen from this curves that CS exhibited the highest swelling capacity, a phenomenon attributed to its hydrophilic nature and the presence of abundant hydroxyl and amine functional groups capable of forming hydrogen bonds with water molecules. These findings are consistent with previously reported data[38–40]. The swelling capacity of CS decreased significantly with increasing pH, a trend similarly observed by Kraaslan et al.[41] and

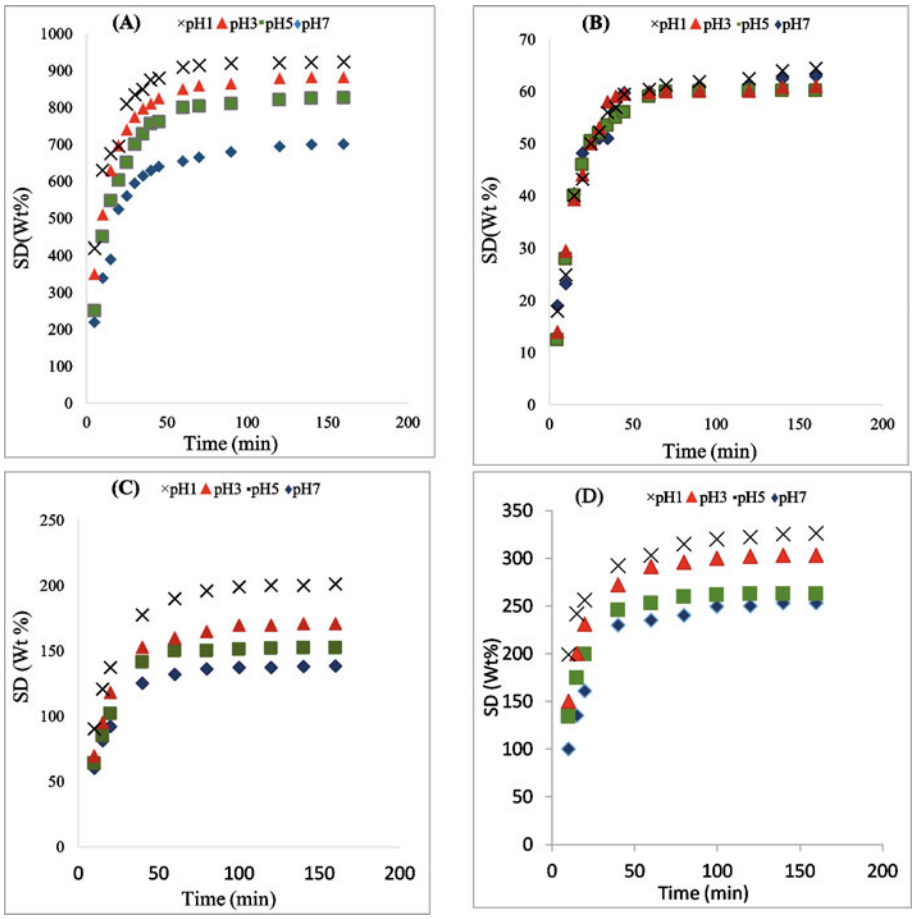

Figure 11. Swelling rate variation as a function of time in different medium pH values for: CS (A); PHEMA (B); CS-*graft*-PHEMA (C); CS/PHEMA (D)

A-ztop et al.[42]. Conversely, PHEMA demonstrated limited swelling capacity, with negligible pH dependence. A maximum swelling was observed in highly acidic media (pH = 1), with reduced swelling in neutral conditions, corroborating prior studies[37, 43].

For the PHEMA-*graft*-CS copolymer, the swelling ranged from 190% to 132% in pH 1 and pH 7 media, respectively. The incorporation of PHEMA, a less hydrophilic polymer, in an equimolar ratio led to a reduction in swelling capacity by over half in both media.

The maximum swelling degree for the blend CS/PHEMA is about 303% and 235% in acidic and neutral media, respectively. Incorporating 50% of PHEMA into the CS matrix resulted in an approximate threefold reduction in CS swelling capacity.

RELEASE KINETICS OF PHACAL

Variation of PhAcAl released percentage(R) versus time from CS PhAcAl -*graft*-PHEMA

Figure 12 illustrates the variation of the PhAcAl released percentage(R) versus time from the CSPhAcAl--*graft*-PHEMA copolymer.

As can be seen from the curve profiles, the maximum of PhAcAl released is 35.00 wt% of the total mass after 120 h reached with CSPhAcAl-*graft*-PHEMA containing 9.52% wt% at pH 7, which is higher than that observed at pH 1 indicating that this system shows better performance. In contrast, the minimum release is obtained with the system containing 3.74 wt% of PhAcAl at pH 1. The significantly higher release percentage at pH 7 compared to pH 1 can be explained by the pH-sensitive nature of chitosan, which is more soluble and swells in acidic conditions but forms a gel-like structure in alkaline or neutral pH, facilitating greater drug diffusion. Furthermore, at pH 7, the ionization of amino groups in chitosan decreases, weakening the interactions between chitosan and PhAcAl, leading to enhanced release.

Variation of PhAcAl released percentage(R) versus time from CSPhAcAl/PHEMA

The curves representing the PhAcAl released percentage versus time in Figure 13, showed that the highest release percentage of PhAcAl is about 44.80 wt%, obtained using the system containing 8.98 wt% of PhAcAl at pH = 7 and also higher than that observed at pH 1, which is 26.55 wt%. The lowest percentages released are 40 wt% at pH = 7 and 18.5 wt% at pH 1 observed for the system containing 15 wt% % of PhAcAl.

The comparison of the performances of the two PhAcAl delivery systems, CSPhAcAl/PHEMA and CSPhAcAl--*graft*-PHEMA, based on the maximum percentage of the drug released, indicates that the CSPhAcAl/PHEMA system achieve the highest PhAcAl released percentage. This suggests that CSPhAcAl/PHEMA system is more effective compared to CSPhAcAl-*graft*-PHEMA system. Furthermore, the released percentage is twice as large at

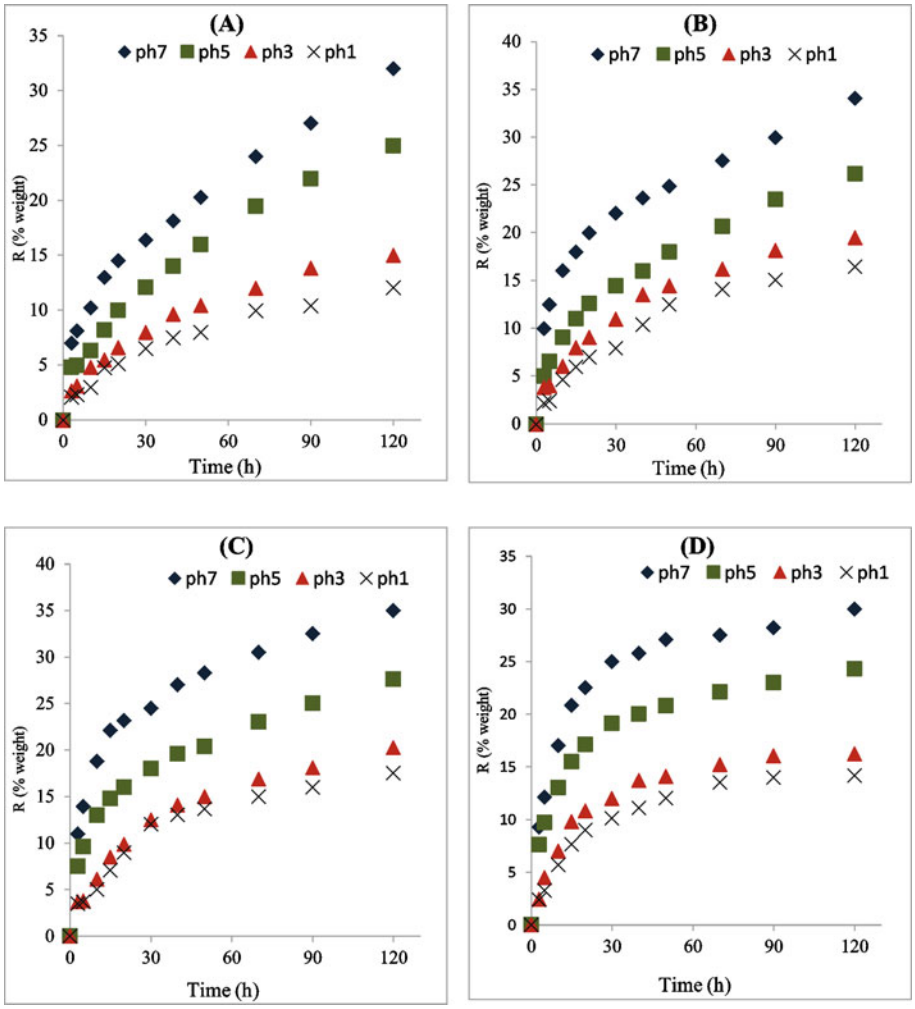

Figure 12. Variation of the PhAcAl released percentage from CSPhAcAl-*graft*-PHEMA: containing 3.74 wt% (A); 8.98 wt% (B); 9.52 wt% (C); and 15.40 wt% (D) of PhAcAl, in different pH environments versus time

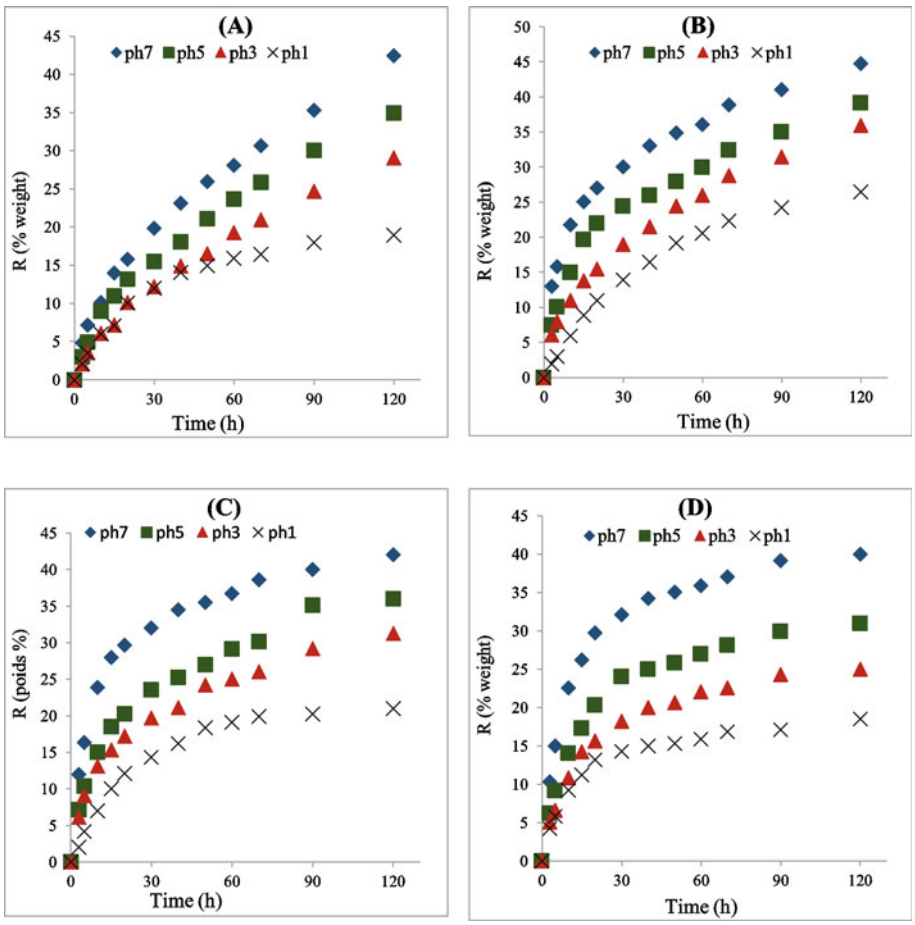

Figure 13. Variation of PhAcAl Release Percentage from CSPhAcAl/PHEMA containing 3.74 wt% (A); 8.98 wt% (B); 9.52 wt% (C); and 15.40 wt% (D) of PhAcAl, in different pH environments versus time

pH 7 as at pH 1 for both systems. The observed higher release percentage of PhAcAl from the CSPhAcAl/PHEMA system can be attributed to the nature of physical blends, where the drug may be more loosely associated with the polymer matrix, facilitating easier diffusion. In the copolymer system, PHEMA is covalently bonded to the chitosan backbone, forming a network that restricts the mobility of the phenylacetaldehyde grafts, reducing the diffusion rate of the drug.

Statistical analysis of the release kinetics

To determine the best-fitting kinetic model, linear regression analysis was applied to the release data according to the different kinetic equations. The calculated kinetic parameters and correlation coefficients (R^2) are summarized in Tables 4 and 5. For the grafted systems, phenylacetaldehyde (PhAcAl) release kinetics were best described by the Korsmeyer–Peppas and Higuchi models for samples containing 3.74 wt% and 9.52 wt% PhAcAl (R^2 = 0.964–0.996), indicating a diffusion-controlled process. At higher PhAcAl contents (8.98 wt%

Table 4. Comparative statistical analysis of the release kinetics models for the CSPhAcAl-*graft*-PHEMA grafted system

pH	R^2 Order 0	R^2 Order 1	R^2 Higuchi Model	Korsmeyer-Peppas model	
				R^2	n
	CSPhAcAl-*graft*-PHEMA3.74				
1	0.8955	0.9317	**0.9921**	0.9843	0.508
3	0.8954	0.9392	0.9952	**0.9961**	0.4893
5	0.9327	0.9757	**0.996**	0.9819	0.4856
7	0.9056	0.981	9.9858	**0.9932**	0.4095
	CSPhAcAl-*graft*-PHEMA8.98				
1	0.8878	0.9127	0.9834	**0.9835**	0.5863
3	0.8657	0.9131	0.9852	**0.9975**	0.4407
5	0.8815	0.9521	0.9869	**0.988**	0.4811
7	0.7752	0.9282	0.8532	**0.9929**	0.3129
	CSPhAcAl-*graft*-PHEMA9.52				
1	0.8098	0.8459	0.9553	**0.9645**	0.4899
3	0.8446	0.8897	**0.9769**	0.9768	0.502
5	0.7788	0.9087	0.8772	**0.989**	0.3361
7	0.6922	0.8531	0.7561	**0.9693**	0.2969
	CSPhAcAl-*graft*-PHEMA15.40				
1	0.744	0.7779	0.9154	**0.9409**	0.4918
3	0.6967	0.7308	0.8723	**0.9021**	0.4811
5	0.6522	0.7707	0.7331	**0.9559**	0.3077
7	0.5904	0.6902	0.6581	**0.9149**	0.305

Table 5. Comparative statistical analysis of the release kinetics models for the CsPhAcAl/PHEMA blended system

pH	R^2 Order 0	R^2 Order 1	R^2 Higuchi Model	R^2 Korsmeyer-Peppas model	
				R^2	n
	CsPhAcAl/PHEMA 3.74				
1	0.819	0.843	**0.964**	0.960	0.593
3	0.958	0.81	0.973	**0.993**	0.688
5	0.944	0.978	**0.988**	0.987	0.631
7	0.940	0.984	0.994	**0.997**	0.568
	CsPhAcAl/PHEMA8.98				
1	0.891	0.913	**0.976**	0.974	0.716
3	0.941	0.964	0.997	**0.999**	0.481
5	0.874	0.912	0.945	**0.975**	0.429
7	0.865	0.907	0.859	**0.989**	0.327
	CsPhAcAl/PHEMA9.52				
1	0.766	0.784	**0.936**	0.925	0.610
3	0.874	0.903	0.973	**0.978**	0.419
5	0.865	0.898	0.943	**0.975**	0.420
7	0.738	0.788	0.742	**0.933**	0.318
	CsPhAcAl/PHEMA15				
1	0.676	0.738	0.814	**0.922**	0.381
3	0.740	0.797	0.900	**0.950**	0.436
5	0.716	0.782	0.875	**0.940**	0.422
7	0.639	0.74	0.750	**0.912**	0.344

and 15 wt%), the Korsmeyer–Peppas model correlated best, and the diffusion exponent ($n < 0.5$) confirmed a Fickian release mechanism, where drug transport is mainly governed by molecular diffusion through the polymeric matrix.

The blended systems also exhibited mixed behavior, for CsPhAcAl/PHEMA3.74, CsPhAcAl/PHEMA8.98, and CsPhAcAl/PHEMA9.52, the release followed the Higuchi model. For CsPhAcAl/PHEMA15, the Korsmeyer–Peppas model with $n < 0.5$ was representative of a purely Fickian diffusion mechanism. The lower values of n at higher pH are representative of the reduced swelling and diffusivity of the polymer matrix at higher pH values, characteristic of diffusion-limited release behavior[24].

CONCLUSION

A comparative study was carried out between two phenylacetaldehyde (PhAcAl) carrier systems, CSPhAcAl-graft-PHEMA and CSPhAcAl/PHEMA blend, at different PhAcAl loadings.

– FTIR and ^{1}H NMR confirmed the formation of the chitosan–Schiff base and successful grafting or blending with PHEMA.

– XRD and DSC analyses revealed the distribution of PhAcAl within the polymer matrices.

–The effect of the PHEMA on swelling properties was assessed. Both carriers showed good swelling in acid pH, which is essential for oral drug delivery systems.

– Notable differences in release behavior were observed between grafted and blended systems. CSPhAcAl/PHEMA blend showed superior performance with optimal release achieved for CSPhAcAl/PHEMA3.74 and CSPhAcAl/PHEMA8.98, giving 26.16 wt% (pH 7) and 35.03 wt% (pH 3), respectively. The grafted system (CSPhAcAl-graft-PHEMA3.74) released smaller amounts (20.34 wt% at pH 7; 6.00 wt% at pH 1).

– The more favorable dissolution from the blend is because of weaker physical interactions and more accessible diffusion channels, whereas the grafted copolymer forms a denser, covalently linked network, which slows down diffusion.

– For the grafted systems, Korsmeyer–Peppas and Higuchi models provided the best regression (R^2 = 0.964–0.996), indicating a Fickian diffusion-controlled mechanism ($n < 0.5$).

– For blended systems, blended behavior was seen: Samples 3.74, 8.98, and 9.52 wt% followed the Higuchi model. The 15 wt% blend followed the Korsmeyer–Peppas model with $n < 0.5$, characteristic of Fickian diffusion.

– These findings indicate that physical blending with PHEMA is a simpler and more tunable approach to the release control of aldehyde drugs, with promise as a strategy for the development of pH-responsive oral delivery systems.

Acknowledgement

The authors gratefully acknowledge the Chemistry Department, College of Science, King Saud University, for their valuable contribution to this work by performing all the analytical measurements and supporting the experimental analysis.

REFERENCES

1. Gao Y. (2018). Introduction and synthesis of polymeric prodrugs. MOJ Bioequivalence & Bioavailability. 5(3), 125–128. DOI: 10.15406/mojbb.2018.05.00092.

2. Duncan, R. & Kopeček, J. (1984). Soluble synthetic polymers as potential drug carriers. In: Polymers in Medicine. Advances in Polymer Science, vol 57, 59–75. Springer, Berlin, Heidelberg. DOI: 10.1007/3-540-12796-8_10.

3. Braatz, D., Cherri, M., Tully, M., Dimde, M., Ma, G., Mohammadifar, E., Reisbeck, F., Ahmadi, V., Schirmer, M. & Haag, R. (2022). Chemical Approaches to Synthetic Drug Delivery Systems for Systemic Applications. Angewandte Chemie – International Edition. 61, e202203942 (1 of 29). DOI: 10.1002/anie.202203942.

4. Ali Alghamdi, A., Al-Soulami, A., Saeed, W.S., Al-Odayni, A., Elsamalali, A., Abdulaziz Al-Owaais, A. & Aouak, T. (2019). Grafting of sulfamethoxazole on acrylic acid−vinyl methyl ketone copolymer using the schiff base reaction−application as a drug delivery system. International Journal of Polymeric Materials and Polymeric Biomaterials, 68(5), 229–242. DOI: 10.1080/00914037.2018.1443929.

5. Xin, Y. & Yuan, J. (2012). Schiff's base as a stimuli-responsive linker in polymer chemistry. Polym. Chem. 3(11), 3045–3055. DOI: 10.1039/c2py20290e.

6. Yang, X., Pan, Z., Choudhury, M.R., Yuan, Z., Anifowose, A., Yu, B., Wang, W. & Wang, B. (2020). Making smart drugs smarter: The importance of linker chemistry in targeted drug delivery. *Med. Res. Rev*. 40(6), 2682–2713. DOI: 10.1002/med.21720.

7. Duceac, I.A. & Coseri, S. (2022). Chitosan Schiff-Base Hydrogels—A Critical Perspective Review. Gels. 8(12). DOI: 10.3390/gels8120779.

8. Antony, R., Arun, T. & Manickam, S.T.D. (2019). A review on applications of chitosan-based Schiff bases. *Int. J. Biol. Macromol*. 129, 615–633. DOI: 10.1016/j.ijbiomac.2019.02.047.

9. Varun Pawariya, Soumik De & Joydeep Dutta (2024). Chitosan-based-Schiff-bases-Promising-materials-for-biomedical-and-industrial-applications. *Carbohydr Polym.* 323, DOI: 10.1016/j.carbpol.2023.121395.

10. Li, M., Wang, H., Chen, X., Jin, S., Chen, W., Meng, Y., Liu, Y., Guo, Y., Jiang, W., Xu, X. & Wang, B. (2020). Chemical grafting of antibiotics into multilayer films through Schiff base reaction for self-defensive response to bacterial infections. *Chem. Engin. J.* 382. DOI: 10.1016/j.cej.2019.122973.

11. Zou, Q., Li, J. & Li, Y. (2015). Preparation and characterization of vanillin-crosslinked chitosan therapeutic bioactive microcarriers. *Int. J. Biol. Macromol*. 79, 736–747. DOI: 10.1016/j.ijbiomac.2015.05.037.

12. Al Khulaifi R.S., AlShehri M.M., Al-Qadsy I., Al Jufareen, M., Saeed, W.S., Badjah-Hadj-Ahmed, A. & Aouak, T.(2023). Breaking the Equilibrium and Improving the Yield of Schiff Base Reactions by Pervaporation: Application to a Reaction Involving n-butylamine and Benzaldehyde. *Separations*, 10(12). DOI: 10.3390/separations10120602.

13. Al-Odayni, A.B.M., Aouak, T., Alghamdi, A., Saeed, W.S., Ouldsmane, M., Karama, U. & Alothman, Z.A. (2018). Ibuprofen grafted on poly(2-hydroxyethylmethacrylate): Synthesis, mass transfer, and in vitro drug release investigations. *J. Polym. Mat. Polym. Biomat*. 67(1), 36–49. DOI: 10.1080/00914037.2017.1297940.

14. Aljubailah, A., Alharbi, W.N.O., Haidyrah, A.S., Al-garni, T.S., Saeed, W.S., Semlali, A., Alqahtani, S.M.S., Al-Owais, A.A., Karmi, A.M. & Aouak, T. (2021). Copolymer involving 2-hydroxyethyl methacrylate and 2-chloroquinyl methacrylate: Synthesis, characterization and in vitro 2-hydroxychloroquine delivery application. *Polymers (Basel),* 13(23). DOI: 10.3390/polym13234072.

15. Zare, M. *et al.* (2021) Phema: An overview for biomedical applications. *Internat. J. Molec. Sci.* 22, Preprint at https: DOI: 10.3390/ijms22126376.

16. Bayramoğlu, G. & Arica, M.Y. (2003) A Novel pH Sensitive Porous Membrane Carrier for Various Biomedical Applications Based on pHEMA/chitosan: Preparation and Its Drug Release Characteristics. in *Macromolecular Symposia,* 203, 213–218. DOI: 10.1002/masy.200351321.

17. Caccavo, D., Cascone, S., Lamberti, G. & Barba, A.A. (2015). Modeling the drug release from hydrogel-based matrices. *Mol. Pharm*. 12(2), 474–483. DOI: 10.1021/mp500563n.

18. Khan, S. & Ranjha, N.M. (2014). Effect of degree of cross-linking on swelling and on drug release of low viscous chitosan/poly(vinyl alcohol) hydrogels. *Polymer Bulletin*, 71(8), 2133–2158. DOI: 10.1007/s00289-014-1178-2.

19. Martinez, A.W., Caves, J.M., Ravi, S., Li, W. & Chaikof, EL. (2014). Effects of crosslinking on the mechanical properties, drug release and cytocompatibility of protein polymers. *Acta Biomat*. 10(1), 26–33. DOI: 10.1016/j.actbio.2013.08.029.

20. Castelli, F., Pitarresi, G. & Giammona, G. (2000). Influence of Different Parameters on Drug Release from Hydrogel Systems to a Biomembrane Model. Evaluation by Differential Scanning Calorimetry Technique. Vol 21, 821–833. DOI: 10.1016/S0142-9612(99)00252-5.

21. Deng, K.L., Zhong, H.B., Tian, T., Gou, Y.B., Li, Q. & Dong, L.R. (2010). Drug release behavior of a pH/temperature sensitive calcium alginate/poly(N-acryloylglycine) bead with core-shelled structure. *Express Polym. Lett*. 4(12), 773–780. DOI: 10.3144/expresspolymlett.2010.93.

22. Mahdi, H.S. & Alshrefi, S.M. (2024). pH-Sensitive Swelling Behavior and Drug Release Kinetics of Chitosan-Modified Cs/HEMA Hydrogels. Preprint. DOI: 10.21203/rs.3.rs-3978283/v1.

23. Heredia, N.S., Vizuete, K., Flores-Calero, M., Pazmiño, V. K., Pilaquinga, F. & Kumar, B., et al. (2022) Comparative statistical analysis of the release kinetics models for nanoprecipitated drug delivery systems based on poly(lactic-co-glycolic acid). *PLoS ONE*, 17(3), e0264825. DOI: 10.1371/journal.pone.0264825.

24. Costa, P. & Lobo, M.J.S. (2001). *Modeling and Comparison of Dissolution Profiles*. *European J. Pharmac. Sci.* 13(2), 123–133. DOI: 10.1016/S0928-0987(01)00095-1.

25. Elmas, A., Akyüz, G., Bergal, A., Andaç, M. & Andaç, Ö. (2020). Mathematical modelling of drug release. *Res. Engin. Structures Mat.* 6(4), 327–350. DOI: 10.17515/resm2020.178na0122.

26. Aouak, T., Saeed, W.S., Al-Hafi, N.M., Al-Odayni, A.B., Alghamdi, A.A. & Bedja, I. (2019). Poly (2-hydroxyethylmethacrylate -co-methylmethacrylate)/lignocaine contact lens preparation, characterization, and in vitro release dynamic. *Polymers* (Basel), 11(5), 917. DOI: 10.3390/polym11050917.

27. Figueiredo, A.G.P.R., Figueiredo, A.R.P., Alonso-Varona, A., Fernandes, S., Palomares, T., Rubio-Azpeitia, E., Barros-Timmons, A., Silvestre, A.J.D., Pascoal-Neto, C. & Freire, C.S.R. (2013). Biocompatible bacterial cellulose-poly(2-hydroxyethyl methacrylate) nanocomposite films. Biomed. Res. Int. Volume 2013, Article ID 698141, 14 pages. DOI: 10.1155/2013/698141.

28. Chauhan, D.S., Mazumder, M.A.J., Quraishi, M.A. & Ansari, K.R. (2020).Chitosan-cinnamaldehyde Schiff base: A bioinspired macromolecule as corrosion inhibitor for oil and gas industry. *Int. J. Biol. Macromol*. 158, 127–138. DOI: 10.1016/j.ijbiomac.2020.04.200.

29. Mucha, M. & Pawlak, A. (2005). Thermal analysis of chitosan and its blends. Thermochim Acta. 427(1-2), 69–76. DOI: 10.1016/j.tca.2004.08.014.

30. Sakurai, K., Maegawa, T. & Takahashi, T. (2000). Glass Transition Temperature of Chitosan and Miscibility of Chitosan/Poly(N-Vinyl Pyrrolidone) Blends. *Polymer*, (41), 7051–7056. DOI: 10.1016/S0032-3861(00)00067-7.

31. Quijada-Garrido, I., Laterza, B., Mazón-Arechederra, J.M. & Barrales-Rienda, J.M. (2006). Characteristic features of chitosan/glycerol blends dynamics. *Macromol. Chem. Phys.* 207(19), 1742–1751. DOI:10.1002/macp.200600230.

32. Dong, Y., Ruan, Y., Wang, H., Zhao, Y. & Bi, D. (2004). Studies on glass transition temperature of chitosan with four techniques. *J. Appl. Polym. Sci.* 93(4), 1553–1558. DOI: 10.1002/app.20630.

33. Nandi, A.K. & Mandal, B.M., Bhattacharyya, S.N. (1985). Miscibility of Poly(Methy1 Acrylate) and Poly(Viny1 Acetate): Incompatibility in Solution and Thermodynamic Characterization by Inverse Gas Chromatography. *Macromolecules* 18, 1454–1460. DOI: 10.1021/ma00149a016.

34. Stroeks, A., Paquaij, R. & Nies, E. (1991). Miscibility behaviour of the system polystyrene poly(p-methylstyrene). Polymer (Guildf). 32(14), 2653–2658. DOI: 10.1016/0032-3861(91)90347-L.

35. Balau, L., Lisa, G., Popa, M.I. Tura, V. & Melnig, V. (2004). Physico-chemical properties of Chitosan films. *Cent. Eur. J. Chem.* 2, 638–647. DOI:10.2478/BF02482727.

36. Beagan, A.M., Aouak, T., AlJuhaiman, L.A., Alodainy, A.M., Saeed, W.S. & Oulad Smane M.(2017) Poly(2-hydroxyethylmethacrylate-co-2-folate ethylmethacrylate) and Folic acid/Poly(2-hydroxyethylmethacrylate) Solid Solution: Preparation and Drug Release Investigation. Polym.- Plastics Technol. Engin. 56(18), 1997–2018. DOI: 10.1080/03602559.2017.1298799.

37. Beagan, A.M., Aouak, T., AlJuhaiman, L.A., Alodainy, A. & Saeed, W.S. (2016). Poly(2-hydroxyethylmethacrylate-graft-folic acid), synthesis, solubility enhancement, and release dynamic of folic acid. *Des Monomers Polym*. 19(6), 479–495. DOI: 10.1080/15685551.2016.1169376.

38. Kyzas, G.Z. & Bikiaris, D.N. (2015). Recent modifications of chitosan for adsorption applications: A critical and systematic review. *Mar Drugs.* 13(1), 312–337. DOI: 10.3390/md13010312.

39. Kyzas, G.Z., Bikiaris, D.N. & Lazaridis, N.K. (2008). Low-swelling chitosan derivatives as biosorbents for basic dyes. *Langmuir.* 24(9), 4791–4799. DOI: 10.1021/la7039064.

40. Kyzas, G.Z., Azizian, S. & Kostoglou, M. (2015). Novel approaches in designing natural/synthetic materials for environmental applications. *Adv. Mat. Sci. Engin.* Volume 2015, Article ID 820854, 1 page. DOI: 10.1155/2015/820854.

41. Karaaslan, A.M., Tshabalala, M.A. & Buschle-Diller, G. (2010). Wood hemicellulose/chitosan-based semi: Interpenetrating network hydrogels: Mechanical, swelling and controlled drug release properties. *Bioresources*, 5(2), 1036–1054. DOI: 10.15376/biores.5.2.1036-1054.

42. Ã-ztop, H.N., Saraydin, D. & Cetinus, Ş. (2002). pH-sensitive chitosan films for baker's yeast immobilization. *Appl. Biochem. Biotech. – Part A Enzyme Engin. Biotech*. 101(3), 239–249. DOI: 10.1385/ABAB:101:3:239.

43. García-Millán, E., Koprivnik, S. & Otero-Espinar, F.J. (2015). Drug loading optimization and extended drug delivery of corticoids from pHEMA based soft contact lenses hydrogels via chemical and microstructural modifications. *Int. J. Pharm*. 487(1-2), 260–269. DOI: 10.1016/j.ijpharm.2015.04.037 .